

A Survey of Modeling and Simulation of Skeletal Muscle

DONGWOON LEE

Autodesk Research, University of Toronto

MICHAEL GLUECK, AZAM KHAN

Autodesk Research

and

EUGENE FIUME, KEN JACKSON

University of Toronto

Muscles provide physiological functions to drive body movement and anatomically characterize body shape, making them a crucial component of modeling animated human figures. Substantial efforts have been expended on developing computational models of muscles for the purpose of increasing realism and accuracy in a broad range of applications, including computer graphics and biomechanics. We survey various approaches that have been employed to model and simulate muscles both morphologically and functionally. Modeling the realistic morphology of muscle requires that muscle deformations be accurately depicted. To this end, several methodologies have been presented, including geometrically-based, physically-based, and data-driven approaches. On the other hand, the simulation of physiological muscle functions aims to identify the biomechanical controls responsible for realistic human motion. Estimating these muscle controls has been pursued through static and dynamic simulations. We review and discuss all these approaches, and conclude with suggestions for future research.

Categories and Subject Descriptors: I.3.7 [Computer Graphics]: Three-Dimensional Graphics and Realism—*Animation*; I.3.5 [Computer Graphics]: Computational Geometry and Object Modeling—*Physically based modeling*

Additional Key Words and Phrases: Human Modeling, Muscle Physiology, Anatomy, Biomechanics

1. INTRODUCTION

Computational human modeling has been an important research topic in many domains: from films and video games, to augmented and virtual reality, in which virtual humans play vital roles. As the value of virtual human models extends to new areas, such as

ergonomics, medicine, and biomechanics, the need for and interest in modeling humans stemming from these new applications grow rapidly. Different approaches to modeling humans respond to different performance requirements. For example, while interactivity is required for real-time applications, visual realism is more desirable in film production. Moreover, physiological and biomechanical accuracy are most crucial in designing medical applications. Despite considerable effort, the immense complexity of the human body continues to make modeling it computationally extremely challenging. Furthermore, our keen perception of human bodies and their movement can make us very critical of even small deviations from expected behavior.

The human body is composed of an intricate and complex anatomical structure which is made up of a variety of interacting tissues. Computational human modeling requires accurate reconstruction of this anatomical structure, the relevant biological and physiological functions, and their mathematical formulation into practical physical and mechanical models. Among the various tissues composing the body, those that form muscles carry out diverse physiological functions and collectively perform body movement. This survey focuses specifically on skeletal muscles because they impart two important features essential for computational human modeling. First, skeletal muscles serve as major body components which make up nearly 50% of total body weight, characterizing the shape of a body and its tone. Second, they provide physiological functions to stabilize body posture and drive body movement. While the former is a key feature for realistic representation of the body which demands accurate modeling of muscle morphology, the latter is crucial for realistic animation of body movement which needs accurate simulation of muscle functions.

Early approaches [Badler and Smoliar 1979; Magnenat-Thalmann 1985] proposed human models based on rigid skeletons. They are straightforward to implement and control, but are only capable of representing simple rigid bodies. Later, muscle and fatty tissue were introduced as additional layers to represent elastic deformation of soft bodies [Chadwick et al. 1989]. However, this muscle model is physically unrealistic and its application is limited to expressing bulging effects over joints. Various researchers have thus devoted significant effort to modeling realistic muscle, focusing on accurate representation of muscle shape and its deformable behaviors. For example, anatomical knowledge has been integrated into constructing muscle geometry [Wilhelms 1997; Scheepers et al. 1997; Nedel and Thalmann 1998; Aubel and Thalmann 2001] and medical imaging techniques have been employed to enhance visual quality [Ng-Thow-Hing and Fiume 1999]. Once muscle geometry is constructed, its deformable behaviors

Authors' addresses: land and/or email addresses.

Permission to make digital or hard copies of part or all of this work for personal or classroom use is granted without fee provided that copies are not made or distributed for profit or commercial advantage and that copies show this notice on the first page or initial screen of a display along with the full citation. Copyrights for components of this work owned by others than ACM must be honored. Abstracting with credit is permitted. To copy otherwise, to republish, to post on servers, to redistribute to lists, or to use any component of this work in other works requires prior specific permission and/or a fee. Permissions may be requested from Publications Dept., ACM, Inc., 2 Penn Plaza, Suite 701, New York, NY 10121-0701 USA, fax +1 (212) 869-0481, or permissions@acm.org.

© 2010 ACM 0730-0301/2010/10-ART106 \$10.00

DOI 10.1145/1559755.1559763

<http://doi.acm.org/10.1145/1559755.1559763>

during muscle contraction need to be described. To this end, a variety of approaches have been proposed: geometrically-based, physically-based, and data-driven approaches. In the biomechanics community, skeletal muscles have also been extensively studied, but most of this work has focused on understanding their mechanical properties and physiological functions for human locomotion. As biomechanical models have been validated through rigorous experiments [Huxley 1957; Zajac 1989], they have begun to draw the attention of graphics researchers, who study simulation of human motions based on computed muscle controls [Komura et al. 2000; Tsang et al. 2005; Lee and Terzopoulos 2006; Lee et al. 2009], ultimately producing realistic human animation. In this survey, we examine and discuss these approaches with respect to two principal features of muscle: muscle deformation and muscle simulation.

This paper is organized as follows. Section 2 gives a brief introduction to anatomical and biomechanical descriptions of muscle, which have been considered in most applications. In section 3, we examine various approaches proposed to model muscle deformation. In section 4, we address muscle control problems and present related simulation models to solve them. Section 5 concludes with a discussion of possible approaches to bridge the efforts of the biomechanical and graphics research communities, working towards a unified model.

2. BACKGROUND

Muscles are the active tissues in the body that generate forces to drive motion. Depending on their physiological functions, muscles can be classified into three types: cardiac, smooth, and skeletal muscle. Cardiac muscles make up the walls of the heart, while smooth muscles constitute the walls of other organs or blood vessels. Both of these two classes of muscle are controlled by the autonomic nervous system and contract without conscious effort. Unlike the first two classes of muscle, skeletal muscle contraction is controlled through the somatic nervous system and, for the most part, is done so consciously. These voluntary contractions produce forces which transfer to the underlying skeleton, resulting in human body movement. Most research in graphics and related fields, such as biomechanics and robotics, has focused on understanding the physiological features and functions of skeletal muscles. In this section, we briefly review both anatomical and biomechanical aspects of skeletal muscle.

2.1 Structural Description

Skeletal muscles are wrapped by the *epiysium*, a dense connective tissue which joins with the tendon. Internally, the muscle is composed of numerous muscle fiber bundles, called *fascicles*, which are separated from one another by a layer of connective tissue known as the *perimysium*. In turn, every fascicle consists of muscle fibers, which are isolated from one another by the *endomysium*. Similarly, each muscle fiber consists of parallel bundles of *myofibrils*. Finally, each myofibril is made up of a serial array of contractile units, called *sarcomeres*, which are responsible for producing the contractions associated with muscles. The hierarchical structure of muscle is illustrated in Figure 1. Although fascicles and fibers are often graphically depicted as circular structures, it is important to note the true mosaic-like space-filling pattern of these components.

Another important component to be considered is tendon. It transmits forces produced by the attached muscle to bone. Tendon connects muscle to bone either at a narrow area or over a wide and flattened area, known as the *aponeurosis*. The attachment of muscle to more stationary bone (i.e., the proximal site) is called the *origin* while the other end to more movable bone (i.e., distal site) is called the *insertion*. Tendons are mostly composed of parallel arrays of collagen fibers closely packed together and have the mechanical property that they are much stiffer than muscles when they are pulled. In addition to force transmission, tendon has a function to passively modulate force during locomotion, providing additional stability (for example, the Achilles tendon during a human stride).

2.2 Muscle Architecture

Muscle architecture refers to the internal arrangement of fascicles within a muscle. A minority of muscles have simple architectures, in which the fascicles are arranged parallel to one another along the length of the muscle. These are typically the larger muscles, such as the biceps brachii or the sartorius. However, most muscles exhibit fascicles with an angular orientation, called the *pennation* angle, between their tendinous attachments and the longitudinal axis of the muscle. Muscles with angular fascicle arrangements are known as *pennate* muscles. Several types of pennation patterns are observed in skeletal muscles, as illustrated in Figure 2. These differences in muscle architecture determine the range of movement and power produced by a muscle. A muscle would contain a greater number of shorter muscle fibers in a pennate configuration than in a parallel configuration. As such, pennate muscles do not shorten as much, but can produce more force than parallel muscles of the same size.

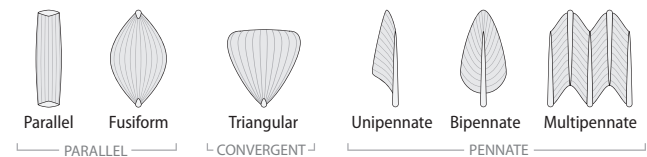


Fig. 2. Exemplary muscle architecture types (adapted from Ng-Thow-Hing [2001])

2.3 Muscle Contraction

Muscle contraction is controlled by the central nervous system; nerve impulses originate from and travel down the motor neurons to the sensory-somatic branch in the muscle. The place where the terminal of a motor neuron and a muscle fiber connect is called the neuromuscular junction. Each motor neuron innervates a set of muscle fibers in which the nerve impulses stimulate the flow of calcium into the sarcomeres, causing their filaments to slide [Jones et al. 2004]. Sarcomeres have protein-based structures composed of high-tensile “thin” filaments of *actin* and “thick” filaments of *myosin*. They are alternatingly stacked on one another and interact via cross-bridges to produce force. The sliding filament and cross-bridge theory [Huxley 1957; Huxley and Simmons 1971] describes the process of muscle contraction. During muscle contraction, the lengths of these filaments remain constant and slide past each other to increase their overlap, producing an overall shortening effect in the muscle, as illustrated in Figure 3. The myosin heads are considered to be elastic elements which oscillate about an equilibrium

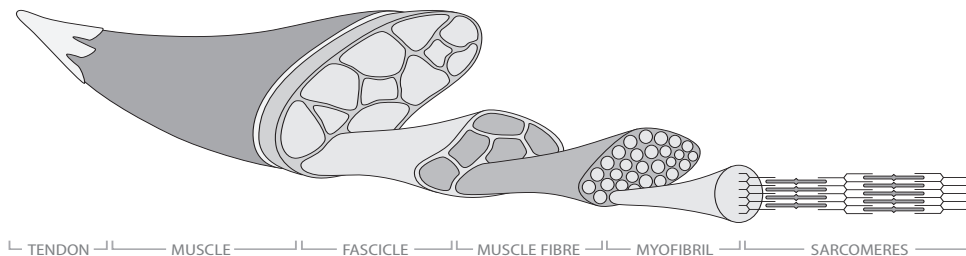


Fig. 1. Major components of the hierarchical muscle structural system (adapted from Ng-Thow-Hing [2001])

position (i.e., position of attachment to the myosin filament) due to biochemical energy. They are linked as the cross-bridges to the myosin binding sites located in the actin filament. When the heads oscillate, they continuously attach or detach from the myosin binding site. When they attach, they exert forces on the actin filaments, causing filaments to slide past each other. Muscle contraction can be classified according to length change or force level. In *isotonic* contraction, muscle length changes while producing force; the muscle either shortens (i.e., *concentric* contraction) or lengthens (i.e., *eccentric* contraction) depending on whether the produced force is sufficient to resist an external load. In *isometric* contraction, muscle length remains unchanged while producing force, as, for example, when holding up an object without moving.



Fig. 3. During concentric muscle contraction, the sarcomere shortens as filaments of myosin pull along the rigid filaments of actin. The more the filaments overlaps, the more the sarcomere thickens (adapted from [Jones et al. 2004]).

2.4 Mechanical Properties

Mechanical properties of muscle associated with force development can be obtained from simple experiments using muscle isolated from tendon [Gasser and Hill 1924]. When the whole muscle is stretched or shortened to several different lengths, the resulting force output is measured and plotted against the length. With no muscle activation, muscle only develops passive restorative force against increased stretching. With muscle activation, muscle contracts and generates active force. The total force is the sum of both active and passive forces (see Figure 4(a)). The active force is found by subtracting the passive force from the total force. The non-linear force-length relationship is consistent with the sliding filament theory of muscle contraction. Another important mechanical property of muscle is the relationship between the velocity at which muscle shortens and the amount of force it produces (plotted in Figure 4(b)). To quantify this relationship, a fully activated muscle is clamped isometrically and then suddenly released to allow shortening against an external load. When there is no load on the muscle, the maximum velocity of shortening is experienced. As the external load increases, the velocity of shortening decreases. This property is known to be associated with the dependence of muscle force on the number of attached cross-bridges [Jones et al. 2004]. During

muscle contraction, cross-bridges attach to produce forces. Since it takes some amount of time for them to attach, as filaments slide past one another more quickly (i.e., muscle shortens with increasing velocity), produced force decreases due to the lower number of attached cross-bridges. Conversely, as the relative velocity of filaments decreases (i.e., muscle shortens with decreasing velocity), more cross-bridges can take time to attach, producing more force.

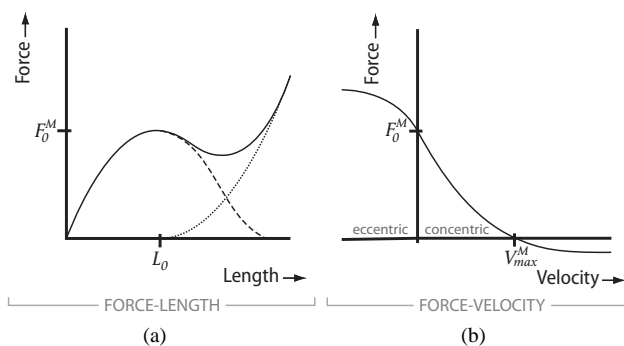


Fig. 4. Mechanical properties of muscles associated with force development (adapted from [Zajac 1989]). (a) A sample force-length plot shows the passive elastic (dotted), active (dashed), and total (solid) force generated by a muscle against its length. F_0^M is the maximum isometric force and L_0 is the rest/optimal length. F_0^M is experienced at L_0 . (b) A sample force-velocity plot shows the changes in force a muscle generates against the velocity of muscle contraction. V_{max}^M is the maximum shortening velocity.

2.5 Mechanical Models

A simple and phenomenological mechanical model (shown in Figure 5(a)) was suggested by Gasser and Hill [1924] to capture the mechanical properties of muscle discussed above. This model has three major components: the series element (SE), the parallel element (PE), and the contractile element (CE). The series element (SE) represents mainly the elastic effects of tendon and intrinsic elasticity within the sarcomere. The parallel element (PE) represents the passive elasticity of the muscle resulting from the penetration of connective tissues into the muscle body. The contractile element (CE) accounts for generation of active force which is dependent on the muscle length, l^M , and the time-varying neural signal, $a(t)$, originating from the central nervous system. The Hill model was later refined by Zajac [1989] to be a dimensionless aggregate or “lumped” model which can be scaled easily to represent any skeletal musculotendon unit. The force components are modeled from the measurement of isolated muscle fibers, which directly

reflect the non-linear properties due to the sliding filaments. While the series elastic element can be lumped with the tendon and removed from the model, pennation effects are directly included into the model. In Zajac's model, muscle length, l^M , tendon length, l^T , muscle force, F^M , and shortening velocity, v^M , are respectively normalized as

$$\tilde{l}^M = \frac{l^M}{l_0^M}, \quad \tilde{l}^T = \frac{l^T}{l_s^T}, \quad \tilde{F}^M = \frac{F^M}{F_0^M}, \quad \tilde{v}^M = \frac{v^M}{v_{max}^M}$$

where l_0^M is optimal muscle length at which F_0^M is developed, l_s^T is tendon rest length, F_0^M is the maximum isometric force of active muscle, and v_{max}^M is the maximum shortening velocity of muscle fibers. The relationship between muscle and musculotendon length is

$$\tilde{l}^{MT} = \tilde{l}^T + \tilde{l}^M \cos(\alpha)$$

where α is the pennation angle (see Figure 5(b)). Normalized active \tilde{F}_{active}^{CE} and passive force \tilde{F}^{PE} can be approximated from the characteristic curves of force-length and force-velocity (shown in Figure 4). Production of contractile force \tilde{F}^{CE} is the \tilde{F}_{active}^{CE} scaled by activation level, $a(t)$, and force-velocity relation, $F_v(\tilde{v}^M)$.

$$\tilde{F}^{CE} = a(t)F_v(\tilde{v}^M)\tilde{F}_{active}^{CE}(\tilde{l}^M)$$

Finally, total force generated by the whole musculotendon unit is

$$\tilde{F}_M = (\tilde{F}^{CE} + \tilde{F}^{PE}) \cos(\alpha) \quad (1)$$

Another commonly used muscle model is the Huxley model [Huxley 1957] which was built by combining the sliding filaments and cross-bridge theory reviewed in Section 2.3. While the Hill model has been used to describe macroscopic behaviors of muscle, the Huxley model has been used mainly to understand the properties of the microscopic contractile elements. To describe muscle contraction, the actin-myosin bonding reaction is expressed using first order kinetics as

$$\frac{dn}{dt} = \frac{\partial n}{\partial t} - v(t)\frac{\partial n}{\partial x} = (1-n)f(x) - ng(x) \quad (2)$$

where $n(x, t)$ is proportional to the number of attached cross-bridges with displacement x at time t , $v(t)$ is the velocity of contraction of a half sarcomere, $f(x)$ is the rate of attachment and $g(x)$ is the rate of detachment. The displacement x is the distance between the equilibrium position and the myosin binding position located in the actin filament. The cross-bridge is defined as the cross-link between the myosin head and the myosin binding position and its behavior is modeled using the Hookean spring with spring constant k . Total force exerted by muscle is calculated by summing forces contributed by each bonded cross-bridge as

$$F(t) = \frac{mkAs(t)}{2l} \int_{-\infty}^{\infty} xn(x, t)dx$$

where m is the number of cross-bridges per unit volume, A is the cross-sectional area of the muscle, $s(t)$ is the sarcomere length and l represents the distance between successive binding positions.

3. MUSCLE DEFORMATION

Muscle is not only a functional unit that drives body movement, it is also a fundamental component in defining the visual appearance

of the human body. Consequently, realistic muscle deformation is needed for high-quality animated human characters. Several approaches have been proposed to model either muscle deformation or muscle-driven body deformation. Their application can be used to simulate different scales of systems, from a single muscle to an entire body. Based on their underlying fundamental methodology, we classify these approaches into three categories: geometrically-based, physically-based, and data-driven approaches.

3.1 Geometrically-Based Approaches

Geometrically-based techniques were employed in early systems because they are practical and efficient. Most proposed approaches have focused on modeling animation effects of muscle contraction, such as bulging or swelling, which can be key factors for skin deformation or facial animation. They have been shown to be successful in modeling simple muscle (e.g., fusiform) but there may not be a straightforward extension to complex muscles [Wilhelms 1997; Scheepers et al. 1997]. Furthermore, since muscle deformation is determined by skeleton arrangement, these techniques have difficulty in achieving a high order of realism from physiological or biomechanical perspectives. Thus, to better handle these problems, muscles are constructed as multiple layers or are often coupled with other physically-based approaches (see Section 3.2).

3.1.1 Space Deformation. Chadwick et al. [1989] employed Free Form Deformations (FFDs) to represent muscle deformation. Articulated skeletons, located inside muscle, transform a surrounding FFD lattice, which in turn represents a muscle shape change. Although FFDs provide simple and fast control, they do not permit direct manipulation. Also, the regular lattice spacing used by FFDs prevents the detailed control needed to produce more complex shapes (see Figure 6). Moccozet et al. [1997] addressed this limitation by introducing Dirichlet Free From Deformations (DFFDs) which are based on a scattered data interpolation technique. They removed the requirement for regularly spaced control points by replacing rectangular local coordinates by generalized natural neighbor coordinates (namely, Sibson coordinates). Given a point, its natural neighbors are collected based on Delaunay and Dirichlet/Voronoi diagrams and its displacement is computed using interpolation. They used a multi-layered deformation model to illustrate hand animation in which the muscle layer is modeled by a DFFD control point set corresponding to a simplified hand topography. In Skeleton-Subspace Deformation (SSD), deformation of surface points is determined by the weighted summation of the associated skeleton coordinate transformations. Muscle bulging or swelling can be modeled by manually defining skeleton subspaces and adjusting weights. Lewis et al. [2000] introduced the Pose-Space Deformation (PSD) by generalizing the interpolation domain, which can be defined by a skeleton or even expression parameters. They improved upon the blending problem, in which neighboring subspaces might incorrectly blend together in SSD, and permitted direct manipulation of the desired deformation.

3.1.2 Parametric and Polygonal Surfaces. Komatsu [1988] used biquartic Bézier surfaces to model body deformation. The Bézier surfaces are patched cylindrically around the skeleton and are jointly controlled to transform the body. Wilhelms [1997] and Scheepers et al. [1997] used a parametric ellipsoid as a basic primitive to model human skeletal muscles. Three principal axes are adjusted to represent the bulging of the muscle belly, while volume is preserved with respect to constrained ratios using predefined relationships among these three axes. Although an ellipsoid is sufficient for modeling simple shapes, such as fusiform muscle, it cannot

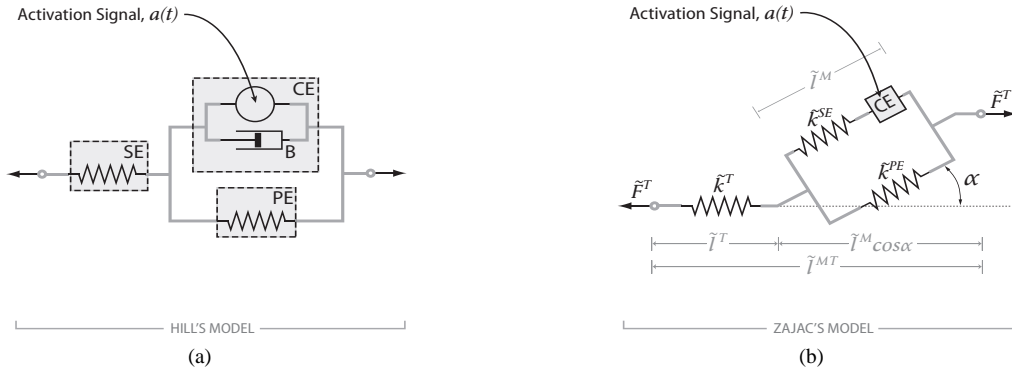


Fig. 5. Mechanical muscle models (adapted from Chen and Zeltzer [1992]). (a) A Hill's model describes the force of a muscle contracting as the sum of three elements, the contractile element (CE), the series elastic element (SE), and the parallel element (PE). (b) Zajac's model extends Hill's model, adding the pennation angle, α , of a muscle fiber.

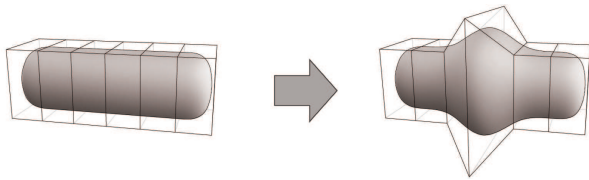


Fig. 6. An exemplary FFD surface is defined by a control lattice around the muscle shape surface. (Left) The FFD surface before deformation. (Right) The FFD surface after deformation.

be easily adapted to model more complex muscle shapes. Scheepers et al. then extended their model to represent multi-belly muscles (e.g., pectoralis) in which n pairs of origin and insertion points are specified and n ellipsoids are laterally aligned along the path within the corresponding pair. Their model is further generalized to represent more complex muscles which are bent and wrapped around anatomical structure (e.g., brachioradialis in the forearm). The straight path between the origin and the insertion point is replaced by a cubic Bézier curve representing the direction of muscle force and ellipses of varying size along this curve to define the volume and shape of the muscle. Dow and Semwal [1993] proposed the generalized cylinder based muscle model, which is represented by a cylinder axis and surrounding cross-sectional slices. The contour of each slice is modeled by B-spline curves and its radius is controlled to express volumetric changes of muscle (see Figure 7). Wilhelms and Gelder [1997] presented a similar approach with the additional flexibility that a cylinder axis can be bent for modeling muscle bent over the joint. Furthermore, the muscle length, width and, thickness are scaled to maintain constant volume.



Fig. 7. An exemplary parametric and polygonal surface: a muscle shape is defined by control of a set of cross-sectional slices. The surface before deformation (left) and after deformation (right).

3.1.3 *Implicit Surfaces.* An implicit surface generated by a set of skeletons, s_i ($i = 1, 2, \dots, n$), with associated field functions, f_i , is defined at the isovalue c by

$$\{P \in \mathbb{R}^3 \mid f(P) = c\} \quad \text{where } f(P) = \sum_{i=1}^n f_i(P)$$

The skeleton, s_i , can be any geometric primitive such as a point, a curve, a parametric surface, etc. The field function, f_i , is generally a decreasing function of the distance from a given point, P , to the associated skeleton (see Figure 8). Based on the type of field function, various implicit surfaces have been developed: blobs, metaballs, soft objects, and convolution surfaces [Blinn 1982; Wyvill and Wyvill 1989; Bloomenthal and Shoemake 1991].

Bloomenthal et al. [1991] used convolution surfaces to model the human hand and arm by approximating bones, muscles, tendons and veins close to the underlying skeletons. Thalmann et al. [1996] presented the multi-layered human model whose body primitives (e.g., muscle, limb, and fatty tissue) are additively constructed from a stick figure skeleton model and coated with the ellipsoidal metaball surfaces. Although the implicit surfaces are smooth and continuous in modeling objects, unwanted blending effects may often occur in modeling deformation over joints. This problem can be avoided by defining neighboring areas between the different skeletons, and specifying how the contributions from them are to be summed (e.g., blending graph [Cani-Gascuel and Desbrun 1997] and weighted blending with the proximity [Singh and Fiume 1998]).



Fig. 8. An exemplary implicit surface is defined by the sum of field functions around associated spherical skeletons. The surface before deformation (left) and after deformation (right).

3.2 Physically-Based Approaches

While geometrically-based models have proven to be sufficient for some graphical applications demanding visually acceptable quality, their inherent simplicity and the need for human intervention often makes it difficult to extend them to represent complex scenes involving dynamics. Furthermore, they lack the physical or mechanical accuracy often required for realistic modeling and simulation. To overcome these deficiencies, many researchers have turned to physically-based approaches in which physics takes care of complicated problems involving muscle dynamics and tissue properties. To model physically-based muscles, the following two problems must be addressed: (1) determining the contractile muscle forces and (2) representing the changing muscle geometry during the contraction. To solve these problems, several muscle models have been proposed based on a variety of computational methods, such as mass-spring systems, FEM (Finite Element Method), and FVM (Finite Volume Method).

3.2.1 Mass-Spring System. An object is modeled by a collection of point masses linked together with massless springs. An elastic force acting on mass i connected by a spring to mass j is given by

$$\mathbf{f}_{ij} = k(|\mathbf{x}_{ij}| - l_{ij}) \frac{\mathbf{x}_{ij}}{|\mathbf{x}_{ij}|}$$

where $\mathbf{x}_{ij} = \mathbf{x}_j - \mathbf{x}_i$, and $\mathbf{x}_i, \mathbf{x}_j$ are the locations of point masses i and j , respectively, l_{ij} is the rest length between them and k is the spring's stiffness. This linear spring model can be generalized by incorporating various types of spring forces, such as angular, bending, and shearing. Each force is derived from an energy minimization principle and serves as a constraint to cause the desired deformation effects.

Chadwick et al. [1989] linked FFD control points to point masses in a mass-spring system, allowing this dynamic system to influence the geometrically-based deformation. By augmenting their FFD-based muscle model with a mass-spring system they were able to represent the viscoelastic properties that articulated skeleton-driven deformation often lacks. Lee et al. [1995] and Albrecht et al. [2003] embedded a muscle layer based on a mass-spring system between the skin surface and the skeleton structure to model facial expressions and the hands, respectively. Spring forces generated by the movement of bones in the skeleton caused the attached skin surface to deform realistically. Nedel and Thalmann [1998] and Aubel and Thalmann [2001] proposed a two-layered muscle model consisting of a line of action and the muscle surface. The line of action is modeled using either a straight line [Nedel and Thalmann 1998] or a 1D mass spring [Aubel and Thalmann 2001] to define the profile of the muscle (e.g., orientation and bone attachment). The skeleton kinematically controls the line of action to deform the surrounding muscle surface based on a mass spring system (see Figure 9(a)). Besides linear springs representing the surface, angular springs have been incorporated to control the volume of the muscle [Nedel and Thalmann 1998]. Ng-Thow-Hing and Fiume [1999; 2001] proposed a more sophisticated model based on anatomical and biomechanical considerations. Their solid muscle is extracted from medical imaging data or cross-sectional sliced images (e.g., Visible Human [Ackerman 1998]) and modeled using volumetric B-splines. For interior details, a muscle fiber architecture is constructed based on digitally scanned fiber data. While a Hill-based model is employed to express the dynamics of muscle fiber, a mass-spring system is used to represent viscoelastic deformation of mus-

cle. Zordan et al. [2004] developed a human torso model to animate breathing motions, such as inhale and exhale. The interplay of ribcage, diaphragm, and abdomen muscle while breathing was described based on respiration mechanics and was simulated using a mass-spring system (see Figure 9(b)). Furthermore, in order to preserve the volume of the human body, pressure forces based on anticipated volume change are incorporated.

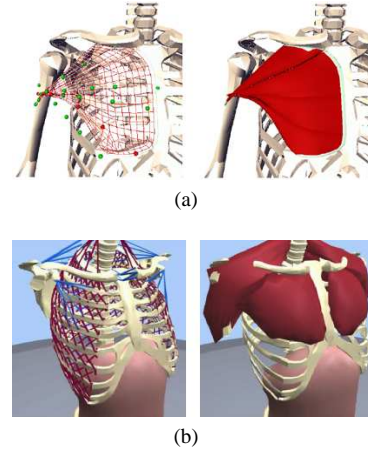


Fig. 9. A mass-spring system is used to simulate behaviors of lines of action and wrapped surfaces of (a) pectoralis muscle [Aubel and Thalmann 2001] and (b) torso model [Zordan et al. 2004]

3.2.2 Finite Element Method (FEM). In the finite element method (FEM), a body is subdivided into a set of domains or finite elements (e.g., hexahedra or tetrahedra in 3D, quadrilaterals or triangles in 2D). Displacements and positions in an element are approximated from discrete nodal values using interpolation functions:

$$\Phi(\mathbf{x}) \approx \sum_i h_i(\mathbf{x})\Phi_i$$

where h_i is the interpolation function for the element containing \mathbf{x} and Φ_i is the scalar weight associated with h_i . There exist many choices for the element type and the interpolation functions. The choice depends on the object geometry, accuracy requirements, and computational budget. Higher order interpolation functions and more complex elements require greater computation per element, but may give a more accurate approximation. For a more complete discussion of the FEM, see [Strang and Fix 2008]. Given a dynamic problem to be solved, equilibrium equations are derived in terms of quantities of interest (e.g., strain or stress) and are expressed as Partial Differential Equations (PDEs). These PDEs are then approximated by the FEM. For example, to represent solid deformation, the total strain energy as the potential energy is carefully designed to express desired material response and then equilibrium equations are derived according to the principle of *virtual work* [Gibson and Mirtich 1997; Nealen et al. 2006]. Resulting algebraic equations form linear or nonlinear system, depending on the specified strain energy. While smaller linear systems can be solved by direct methods (e.g., Gaussian Elimination), large or nonlinear systems require iterative methods (e.g., Conjugate Gradient or Newton's method) [Press et al. 1992].

Chen and Zeltzer [1992] proposed a biomechanical approach by integrating a Hill-based muscle model into a linear elastic solid model. Active muscle forces are approximated as parametric functions and embedded into selected edges between vertices of a FEM-based solid. While they animated flexion of muscles, they emphasized the biomechanical validity of their model by comparing it to experimental measurements, such as the force-length and quick-release properties. Zhu et al. [2001] employed Stern's muscle model [Stern 1974] in which simplified behaviors of bone-joint-muscle complexes are described. Both works employed a linear elastic material model for connective passive tissues of muscle, which is computationally efficient but valid only for infinitesimal deformation. In contrast, Hirota et al. [2001] and Lemos et al. [2001] adopted nonlinear material models that allowed the robust representation of large deformations. Hirota et al. combined the Mooney-Rivlin model [Mooney 1940], the Veronda model [Veronda and Westmann 1970] and the fiber-reinforcement material model [Klischab and Lotza 1999] to express passive response of tissues during body contact. Lemos et al. [2001] used a rubber-like material model (e.g., hyperelastic material) and explicitly aligned Hill-based muscle forces to fiber orientations within the finite elements. In biomechanics, FEM has been widely investigated for studying skeletal muscles. Various muscle models have been proposed to analyze and predict accurate strain distribution of muscle during contraction and its functional properties. Yucesoy et al. [2002] modeled the mechanical behavior of skeletal muscle as the interaction between the intracellular domain (i.e., muscle fibers) and extracellular matrix domain (i.e., connective tissues). Thus, muscle geometry is represented by two separate meshes that are elastically linked to account for the force transmissions between these two domains. Silvia and Delp [2005] developed a way to represent complex muscle geometry and architecture (see Figure 10(a)). A variation of the moment arms of fibers is modeled and the predicted changes to muscle shape are compared to magnetic resonance images. Tang et al. [2009] proposed a constitutive muscle model in which active contraction of muscle fibers and hyperelastic material properties are coupled using the strain energy approach. They demonstrated different types of contractions, such as concentric and eccentric contraction, and effects of muscle geometry and fiber orientation on the stress distribution. [Gielen et al. 2000; Oomens et al. 2003] incorporated the Huxley model to represent contractile properties of skeletal muscle. The Huxley equations (Equation 2) are approximated using a Distributed Moments approach [Zahalak 1981] and combined with the constitutive equation describing nonlinear and incompressible material response.

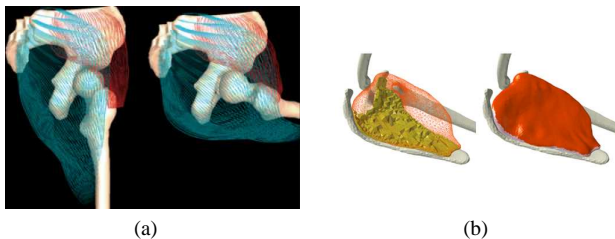


Fig. 10. Physically-based Approaches: (a) gluteus maximus and medius muscle models with the hip extension and flexion (based on FEM, [Blemker and Delp 2005]) and (b) subscapularis muscle model attached to scapula bone model (based on FVM, [Teran et al. 2005])

3.2.3 Finite Volume Method (FVM). As with FEM, the finite volume method approximates PDEs by algebraic equations. For the integration of conserved variables in PDEs, volume integrals are converted to surface integrals using the divergence theorem. These terms are then evaluated as fluxes at the surfaces of each finite volume. For example, to compute the internal force \mathbf{f} at node \mathbf{x}_i , we use

$$\mathbf{f}_i = \frac{d}{dt} \iiint_{\Omega} \rho \mathbf{v} d\mathbf{x} = \frac{d}{dt} \iint_{\partial\Omega} \mathbf{t} dS = \frac{d}{dt} \iint_{\partial\Omega} \boldsymbol{\sigma} \mathbf{n} dS$$

where ρ is the density, \mathbf{v} is the velocity, \mathbf{t} is the surface traction on $\partial\Omega$, $\boldsymbol{\sigma}$ is the stress tensor, and \mathbf{n} is the surface normal. For a more complete discussion of the FVM, see [LeVeque 2002].

Teran et al. [2003; 2005] proposed a FVM-based approach to simulate deformable behavior of skeletal muscles (shown in Figure 10(b)). They argue that FVM inherently requires less computation and memory usage than FEM does. To represent highly nonlinear material response of muscle, they used the sophisticated constitutive model similar to [Hirota et al. 2001]. Furthermore, they incorporated anisotropic properties based on fiber architecture, which are modeled using the B-spline solid technique [Ng-Thow-Hing and Fiume 1999].

3.3 Data-Driven Approaches

In contrast to many methods involving the modeling of physical human components and processes, some data-driven approaches forego anatomical mechanisms and directly model the skin shape, deformed by the underlying muscle, of a human in plausible poses. Data is captured on the surface of subjects usually with markers on the skin by a motion capture system or a range scanning device. Several techniques are then used to generate a new skin surface given a novel skeleton pose. Although such data-driven approaches are relatively new, several key papers have already shown the power of this technique.

Early work by Min et al. [2000] is based on the observation that skin shape in a human scan is determined by the underlying skeleton and muscle, and uses an anatomically-based approach having layers of skeleton, muscle, and skin. Moving the skeleton deforms the isosurface muscle in a volume-preserving fashion, which in turn deforms the skin layer. The upper body was modeled and the resulting animation showed realistic arm bending and stretching. Another approach to arm animation used several exemplary arm shapes [Sloan et al. 2001] and a unique interpolation scheme using linear and radial basis functions to create a continuous range of well-behaved poses.

As example poses of human subjects became more accessible, more ambitious systems were created [Ma et al. 2004]. The range scanning technique, a person poses for a short time as a scanner creates tens of thousands of data points on the surface of the subject at a density of just a few millimeters. Allen et al. [2002] created a high qualityposable upper body model from range scan data together with many correspondence markers. This work was later expanded [Allen et al. 2003], to accommodate the large CAESER (Civilian American and European Surface Anthropometry Resource project) database of whole-body range scans, resulting in a compelling system with several desirable features. Morphing by interpolating between registered scans or fitting a model to a sparse marker set are two significant outcomes of this technique. The technique also supported transferring texture, surface data or

animation between models to correct scanning problems, alter the appearance, or to animate the characters. Multiple correlated parameters could be modified, such as a person's weight or height, or statistically correct human shapes could be preserved when locally modifying a character part, for example, lengthening an arm.

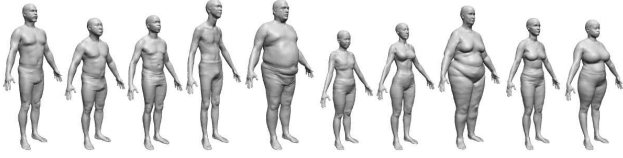


Fig. 11. Data-driven approach: statistical model [Allen et al. 2003]

There are many steps involved in creating the reconstruction and parameterization of the CAESER data sets. Previous techniques, which were used primarily on morphable face models, were based on cylindrical mappings that could not be adapted to a complex branching object, like the complete human body. This work used an artist-generated template object together with a non-rigid registration technique to create a vertex correspondence between a set of skin surfaces that have substantial variation in shape, but a common overall human structure. An energy-minimization approach was used with a weighted sum error objective function that combines distance to a template object, smoothness, and marker distance.

Seo and Thalmann [2003] presented a similar template-based system with additional tailoring parameters to generate new, instantly animatable, high-quality human forms, ideal for fashion design. An alternate technique uses many silhouettes from a video stream instead of range scan data to formulate the human shape in a re-animatable form [Sand et al. 2003]. Anguelov et al. [2005] extended this work, focusing on representing muscle deformation resulting from articulated body motion, to perform Shape Completion and Animation of People (SCAPE), by using separate models for pose deformation and for body shape variation. By decoupling the skeleton (rigid) deformation from the muscle (non-rigid) deformation, the formulation, identification of the model, and the efficiency of the learning algorithms are all improved. A limitation is that a single muscle deformation model is used for all people so that a more muscular person may not exhibit as much muscle deformation as they should.

Data-driven modeling of skin and muscle deformation was further refined by Park and Hodgins [2006; 2008] by modeling static deformations, as a function of skeleton pose, and dynamic deformations, as a function of the acceleration of each body part. Animated motions of an actor were captured using a high density of 350 markers, while performing slow motions and then fast motions. The two classes of deformation were then modeled and new animations could be generated from more typical marker counts (40 to 50 markers) in additional motion-capture sessions. Although this approach still has the limitation of being skeleton-driven and does not express muscle motion without joint angle changes, it does produce very high quality results.

4. CONTROL AND SIMULATION

While Section 3 examined various approaches proposed to represent deformable behavior of skeletal muscles, this section reviews

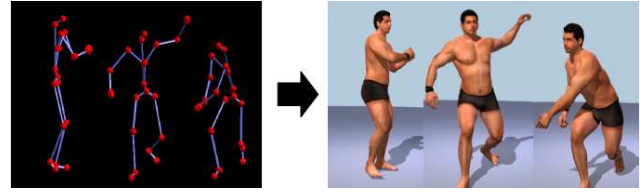


Fig. 12. Data-driven approach: motion-capture [Park and Hodgins 2008]

numerous simulation models which were developed to control muscle functions, producing realistic human movement. In general, the musculoskeletal system is modeled as a combination of three sub-models: activation dynamics, contraction dynamics, and skeleton dynamics. Activation dynamics describe dynamic relations between the neural excitation and muscle activation, which is often modeled using first order Ordinary Differential Equations (ODEs) as

$$\frac{da_j}{dt} = (u_j - a_j) \left(\frac{u_j}{\tau_{act,j}} + \frac{1 - u_j}{\tau_{deact,j}} \right) \quad (3)$$

where u_j , a_j , $\tau_{act,j}$ and $\tau_{deact,j}$ are the neural excitation, muscle activation, activation time constant and deactivation time constants of muscle j , respectively. Contraction dynamics relates muscle activation to resulting muscle forces by taking into account physiological features of muscle, such as fiber arrangement and passive tissue properties. A Hill model is commonly used to model contraction dynamics (see Section 2.5). Skeleton dynamics accounts for the relationship between muscle forces, external constraints, and resulting skeletal motions:

$$M(\mathbf{q})\ddot{\mathbf{q}} + c(\mathbf{q}, \dot{\mathbf{q}}) + g(\mathbf{q}) - S(\mathbf{q})\mathbf{f}_{ext} = R(\mathbf{q})\mathbf{f}_{mt} \quad (4)$$

where \mathbf{q} , $\dot{\mathbf{q}}$, $\ddot{\mathbf{q}}$ are vectors of the generalized coordinates of joints, velocity, and acceleration, respectively. $M(\mathbf{q})$ is the generalized inertia matrix, $c(\mathbf{q}, \dot{\mathbf{q}})$ is the vector of generalized Coriolis and centrifugal forces and $g(\mathbf{q})$ is the vector of the generalized gravitational forces. $S(\mathbf{q})$ and $R(\mathbf{q})$ denote the geometric transformation matrices of the generalized external forces (\mathbf{f}_{ext}) and musculotendon forces (\mathbf{f}_{mt}) to the joint forces, respectively. Upon generating skeletal motions using (4), driving muscle forces can be computed using either manually-specified profiles (e.g., handcrafted curves [Chen and Zeltzer 1992], sinusoid [Tu and Terzopoulos 1994; Zordan et al. 2004], and key-framed control [Teran et al. 2003]) or computationally-predicted values of muscle activation (e.g., [Tsang et al. 2005; Lee and Terzopoulos 2006; Sueda et al. 2008]). In biomechanics, the computation of muscle functions has been systematically studied through rigorous experiments, and a variety of simulation models have been developed and validated against experimental data. As the complexity of desired motion increases or more realistic representations are required in human animation, the usage of these simulation models becomes more advantageous due to their reliability, consistency, and accuracy.

However, determination of muscle functions is challenging because it is complicated by the high redundancy of the human muscle system: the number of contributing muscles is greater than the number of degrees of freedom specifying skeletal motion, leading to an underdetermined problem. This problem is often solved by using optimization approaches, which are generally classified into static and dynamic optimization. They are generally formulated into finite, constrained, and nonlinear optimizations of the control parameterization, which are commonly solved by sequen-

tial quadratic programming methods [Nocedal and Wright 2006]. We briefly describe below these two optimization approaches and review simulation models based on them.

4.1 Static optimization

Static optimization (also referred to as inverse dynamics) takes non-invasive measurements of body motions, such as position, velocity, acceleration, and external loads, as inputs to (4) to calculate muscle forces (see Figure 13). An instantaneous motion of the skeleton at each time instant is translated into algebraic equations in which desired criteria are specified as a set of constraints (e.g., $0 \leq F_{mt} \leq F_{mt}^{max}$) or objective functions. As an objective function, minimizing total muscle force or activation amplitude [Crowinshield and Brand 1981] is commonly adopted:

$$J = \sum_{i=1}^n \left(\frac{F_{mt,i}}{PCSA_i} \right)^2 \quad (5)$$

where $F_{mt,i}$ is the force applied by muscle i at time instant t , $PCSA_i$ is the cross-sectional area of muscle i , and n is the number of muscles. In static optimization, as there is no dynamic dependency between muscle forces at different time instants, time integration is not necessary, which makes the problem computationally simpler. However, it is difficult to integrate muscle physiology (e.g., excitation and activation dynamics) and the objective of the motor tasks (e.g., maximum height jumping). Furthermore, its validity is highly dependent on the accuracy of the experimental measurement of motions.

Komura et al. [1997; 2000] computed muscle activation from key-framed postures of human lower extremities while minimizing total torque changes and activation amplitude. Their model was further extended to consider some physiological features, such as muscle fatigue and injury [Komura et al. 2000]. Tsang et al. [2005] presented a musculotendon model of the human hand and forearm. Their model features both inverse and forward simulation. Given motion capture data or key-framed animation, an optimal set of muscle activations is determined using the static optimization method and then taken as input to forward simulate the model to achieve the desired pose or motion. Their optimization criteria are formulated based on the minimization of the kinematic error between computed and measured motion, and the total amount of muscle contraction. Lee and Terzopoulos [2006] proposed a hierarchical approach to simulate the head and neck system (see Figure 14(b)), which is controlled by a higher-level voluntary sub-controller and a lower-level reflex sub-controller. The voluntary controller generates feedforward neural signals with respect to the desired pose, muscle tone (i.e., stiffness), and feedback gains based on monitored current motion. Upon their receipt, the reflex controller determines activation and co-activation of muscles, and modulates strain and strain rate of muscles in response to their current state. An artificial neural network is employed to model these voluntary controllers and they are trained offline to precompute feedforward signal functions of the target pose. This approach was extended to simulate a complete human upper body by integrating trunk and arm models [Lee et al. 2009]. As well as the muscle-based skeletal dynamics, a physics-based soft tissue simulator was incorporated to represent realistic flesh deformation during body movement. Kim et al. [2006] optimized several motion tasks based on the hypothesis that total energy consumption governs human motion. The energy is described as the heat generated by muscle and formulated in joint space. Optimal joint kinematic profiles are computed while minimizing total energy expended at

each time interval. Sueda et al. [2008] presented a musculotendon simulation of a human hand, in which behaviors of muscles and tendons are governed by spline-based strand dynamics (see Figure 14(a)). The strand dynamics are formulated by coupling muscle contraction and constraint forces based on routing of muscle and tendons. The optimal muscle activation is computed with respect to minimized total activation and proper damping.

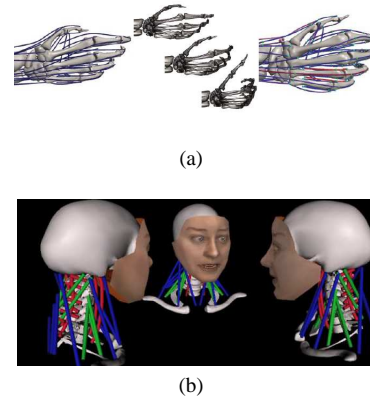


Fig. 14. Static optimization: (a) musculotendon simulation for hand ([Sueda et al. 2008]) and (b) neuromuscular simulation for head and neck ([Lee and Terzopoulos 2006])

4.2 Dynamic optimization

Dynamic optimization (also referred to as forward dynamics) is generally formulated by combining (1), (3) and (4), taking muscle excitation as inputs to produce body motion and then determining the optimal excitation trajectory while satisfying performance criteria (see Figure 15). While static optimization only accounts for each time instant, dynamic optimization considers the entire duration of movement, requiring the time integration of (4). Thus, dynamic optimization is much more computationally expensive than static optimization. However, in contrast to static optimization, physiological, and time-dependent properties can be incorporated. Also, desired motor tasks can be formulated as performance criteria, such as minimum-time kicking [Hatze 1976], maximum-height jumping [Pandy et al. 1990], and maximum-distance throwing [Hubbard and Alaways 1989]. Anderson and Pandy [2001a; 2001b] employed the minimization of metabolic energy expenditure [Umberger et al. 2003] per unit distance which is assumed to characterize human gait during normal walking. Anderson and Pandy [2001b] showed that static optimization and dynamic optimization lead to virtually similar results in predicting muscle forces and joint contact forces during normal human walking. They argued that this similarity is because minimizing muscle fatigue at each time instant is roughly the same as minimizing metabolic energy expended per unit distance traveled over the complete gait cycle. Also, they pointed out that physiological properties, such as the force-length-velocity properties of muscle and activation dynamics, had little influence on static optimization.

5. DISCUSSION AND CONCLUSION

We have reviewed a variety of approaches for modeling muscle deformation and simulation of muscle functions. For modeling

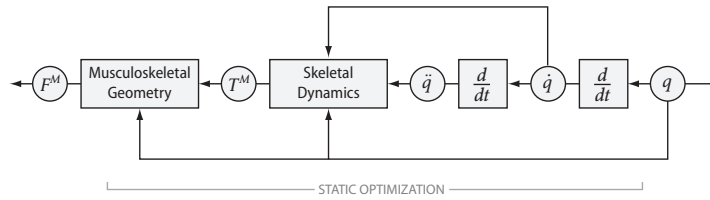


Fig. 13. Static optimization (or inverse dynamics) pipeline. Body motions are prescribed as inputs and optimal muscle forces are determined as outputs (Adapted from [Zajac and Gordon 1989]).

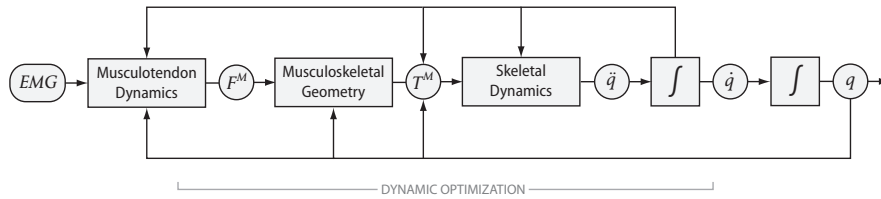


Fig. 15. Dynamic optimization (or forward dynamics) pipeline: muscle excitation is prescribed as inputs and the resulting skeletal motion is used to determine optimal excitation (adapted from [Zajac and Gordon 1989]).

muscle deformation, geometrically-based approaches prevailed in early work because of their simplicity and efficiency. Although these techniques produce results that have limited accuracy and realism, they may still be appropriate solutions for some real-time applications, in that they provide intuitive and easy controls for designers to produce animations. On the other hand, physically-based approaches augmented with biomechanical and physiological considerations provide a high degree of visual quality and accuracy in modeling muscles. Despite high computational demands, their feasibility in applications continues to expand thanks in part to increasing computing power. Data-driven muscle and skin deformation modeling has advanced significantly in recent years. Only a few components in addition to those proposed by Park and Hodgins [2008] are still needed to produce a complete system for computer graphics applications. Isometric muscle effects without joint-angle changes is still an outstanding problem as is the ability to drive existing models from new actors, which was available in other previous works. We are optimistic that, for the purposes of computer animation, a complete system can be created that is entirely data-driven.

For simulation of muscles, we have reviewed static and dynamic optimization, which can be viewed as complementary approaches. If external forces and body motions can be accurately measured, static optimization is preferred because it provides a practical and computationally efficient solution for estimating muscle forces. On the other hand, dynamic optimization offers a more reliable and stable solution. Also, if time-dependent performance criteria must be considered (e.g., maximum-height jumping) or if the aim is to investigate the influence of musculoskeletal structures on the function and performance of a motor task, dynamic optimization must be used.

While significant progress has been made to date, there are still many issues for future work. We offer some suggestions which

could be helpful for enhancing visual realism and accuracy in modeling muscle and ultimately the complete human.

Firstly, many researchers have focused primarily on modeling muscles with simple internal architecture (e.g., parallel and fusiform) rather than complex pennate muscles. Moreover, suggested muscle models are often oversimplified by neglecting nonuniformity and irregularity that is clearly present in the architecture of real muscle specimens. The reason for this may be due to the limited availability of data and unknown physiological properties. However, in order to enhance anatomical and physiological accuracy, this complexity must be considered. Some invasive assessment techniques, such as those proposed by Agur et al. [2003] and Wu et al. [2007], could be incorporated (see Figure 16). In addition to accurate reconstruction of muscle morphology, the effect of complex muscle structure on muscle deformation and physiological functions needs to be studied further. Validation against experimental measurements should be attempted.

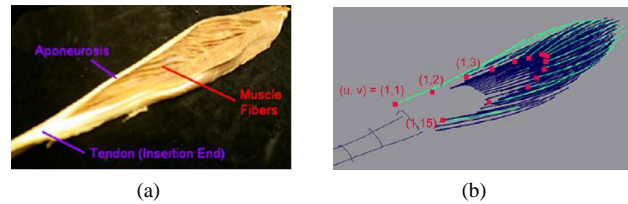


Fig. 16. Digitization and reconstruction of muscle fibers: (a) sagittally dissected ECRB muscle and (b) reconstruction of muscle fibers using digitization ([Wu et al. 2007])

Secondly, there is a need to solve contact problems which occur in muscle groups or between muscles and the underlying skeleton. This problem has been largely overlooked in previous approaches which have presented models for the simulation of a

single muscle in isolation or simple muscle-skeleton dynamics. Some researchers (e.g., [Lee and Terzopoulos 2006; Lee et al. 2009]) have used multiple muscles to coordinate body movements, but they did not address the issues associated with collision or contact between muscles. This is a crucial omission, since most of our muscle systems, such as biceps, triceps, and quadriceps, are grouped together and intertwined. Furthermore, for realistic modeling and accurate simulation of body movement, a solution to the contact problem within muscle groups would produce a significant advancement in this area.

Thirdly, biomechanics-based techniques could enhance visual realism and accuracy of controls in human animation. In biomechanics, significant progress has been made in understanding human movements through rigorous data capture and analysis. Recently, some simulation models have been introduced to provide more accurate, realistic, and automated controls for muscle-based animations [Komura et al. 2000; Tsang et al. 2005; Lee and Terzopoulos 2006; Lee et al. 2009]. They have shown that the inclusion of biomechanical approaches can produce more accurate and realistic human models. This work is promising for various applications, such as ergonomics and medicine. However, biomechanical models are often too computationally expensive for use in graphics applications. Some simplification or approximation may be needed to obtain the efficiency needed for graphics applications.

Lastly, some physiological considerations could provide additional expressive controls in human modeling. For example, animation of human walking could be varied by specifying physiological or pathological effects, such as fatigue, which is related to the calcium level inside muscles. Also, restriction of activation range of certain muscles or muscle fibers could be used to model muscle related injury or disease. Although they can be manually controlled [Tsang et al. 2005], simulation against external loads could yield promising results, which could be useful not only for video games, but also for ergonomics and rehabilitation applications.

Ultimately, a unified model, scalable from visually realistic interactive systems to highly accurate offline patient-specific diagnostics systems, is the holy grail of this research area. While much still needs to be learned about detailed muscle architecture, human variation, and human muscle coordination strategies, progress is being made both in computer graphics research and biomechanics research. We believe that more extensive collaboration between these research communities will result in great advancements towards a unified model.

REFERENCES

- ACKERMAN, M. 1998. The visible human project. In *Proc. IEEE*. Vol. 86. 504–511.
- AGUR, A. M., NG-THOW-HING, V., BALL, K. A., FIUME, E., AND MCKEE, N. H. 2003. Documentation and three-dimensional modelling of human soleus muscle architecture. *Clinical Anatomy* 16, 4, 285–293.
- ALBRECHT, I., HABER, J., AND SEIDEL, H.-P. 2003. Construction and animation of anatomically based human hand models. In *SCA '03: Proceedings of the 2003 ACM SIGGRAPH/Eurographics symposium on Computer animation*. Eurographics Association, Aire-la-Ville, Switzerland, Switzerland, 98–109.
- ALLEN, B., CURLESS, B., AND POPOVIĆ, Z. 2002. Articulated body deformation from range scan data. *ACM Trans. Graph.* 21, 3, 612–619.
- ALLEN, B., CURLESS, B., AND POPOVIĆ, Z. 2003. The space of human body shapes: reconstruction and parameterization from range scans. In *SIGGRAPH '03: ACM SIGGRAPH 2003 Papers*. ACM, New York, NY, USA, 587–594.
- ANDERSON, F. C. AND PANDY, M. G. 2001a. Dynamic optimization of human walking. *Journal of Biomechanical Engineering* 123, 5, 381–390.
- ANDERSON, F. C. AND PANDY, M. G. 2001b. Static and dynamic optimization solutions for gait are practically equivalent. *Journal of Biomechanics* 34, 2, 153–161.
- ANGUELOV, D., SRINIVASAN, P., KOLLER, D., THRUN, S., RODGERS, J., AND DAVIS, J. 2005. Scape: shape completion and animation of people. *ACM Trans. Graph.* 24, 3, 408–416.
- AUBEL, A. AND THALMANN, D. 2001. Interactive modeling of the human musculature. In *Proceedings of Computer Animation*. 125–135.
- BADLER, N. I. AND SMOLIAR, S. W. 1979. Digital representations of human movement. *ACM Comput. Surv.* 11, 1, 19–38.
- BLEMKER, S. S. AND DELP, S. L. 2005. Three-dimensional representation of complex muscle architectures and geometries. *Annals of Biomedical Engineering* 33, 5, 661–673.
- BLINN, J. F. 1982. A generalization of algebraic surface drawing. *ACM Trans. Graph.* 1, 3, 235–256.
- BLOOMENTHAL, J. AND SHOEMAKE, K. 1991. Convolution surfaces. In *SIGGRAPH Computer Graphics*. 251–256.
- CANI-GASCUEL, M.-P. AND DESBRUN, M. 1997. Animation of deformable models using implicit surfaces. *IEEE Transactions on Visualization and Computer Graphics* 3, 1, 39–50.
- CHADWICK, J. E., HAUMANN, D. R., AND PARENT, R. E. 1989. Layered construction for deformable animated characters. In *SIGGRAPH Computer Graphics*. 243–252.
- CHEN, D. T. AND ZELTZER, D. 1992. Pump it up: computer animation of a biomechanically based model of muscle using the finite element method. In *SIGGRAPH Computer Graphics*. 89–98.
- CROWNINSHIELD, R. AND BRAND, R. 1981. A physiologically based criterion of muscle force prediction in locomotion. *Journal of Biomechanics* 14, 11, 793–801.
- DOW, E. AND SEMWAL, S. 1993. A framework for modeling the human muscle and bone shapes. In *Proceedings of the Third International Conference on CAD and Computer Graphics*. 110–113.
- GASSER, H. AND HILL, A. 1924. The dynamics of muscular contraction. In *Royal Society of London Proceedings*. 398–437.
- GIBSON, S. F. F. AND MIRTICH, B. 1997. A survey of deformable modeling in computer graphics. Tech. rep., Mitsubishi Electric Research Laboratories.
- GIELEN, A. W. J., OOMENS, C. W. J., BOVENDEERD, P. H. M., ARTS, T., AND JANSSEN, J. D. 2000. A finite element approach for skeletal muscle using a distributed moment model of contraction. *Computer Methods in Biomechanics and Biomedical Engineering* 3, 3, 231–244.
- HATZE, H. 1976. The complete optimization of a human motion. *Mathematical Biosciences* 28, 1–2, 99–135.
- HIROTA, G., FISHER, S., STATE, A., LEE, C., AND FUCHS, H. 2001. An implicit finite element method for elastic solids in contact. In *Computer Animation*.
- HUBBARD, M. AND ALAWAYS, L. 1989. Rapid and accurate estimation of release conditions in the javelin throw. *Journal of Biomechanics* 22, 6–7, 583–595.
- HUXLEY, A. F. 1957. Muscle structure and theories of contraction. *Progress in Biophysics and Biophysical Chemistry* 7, 255–318.
- HUXLEY, A. F. AND SIMMONS, R. M. 1971. Proposed mechanism of force generation in striated muscle. *Nature* 233, 533–538.

- JONES, D., HAAN, A. D., AND ROUND, J. 2004. *Skeletal Muscle – Form and Function*. Churchill Livingstone.
- KIM, J. H., ABDEL-MALEK, K., YANG, J., AND MARLER, R. T. 2006. Prediction and analysis of human motion dynamics performing various tasks. *International Journal of Human Factors Modelling and Simulation 1*, 1, 69–94.
- KLISCHAB, S. M. AND LOTZA, J. C. 1999. Application of a fiber-reinforced continuum theory to multiple deformations of the annulus fibrosus. *Journal of Biomechanics 32*, 10, 1027–1036.
- KOMATSU, K. 1988. Human skin model capable of natural shape variation. *The Visual Computer 3*, 5, 265–271.
- KOMURA, T., SHINAGAWA, Y., AND KUNII, T. 1997. A muscle-based feed-forward controller of the human body. *Computer Graphics Forum 16*, 3, C165–C176.
- KOMURA, T., SHINAGAWA, Y., AND KUNII, T. 2000. Creating and retargeting motion by the musculoskeletal human body model. *The Visual Computer 16*, 5, 254–270.
- LEE, S.-H., SIFAKIS, E., AND TERZOPOULOS, D. 2009. Comprehensive biomechanical modeling and simulation of the upper body. *ACM Trans. Graph. 28*, 4, 1–17.
- LEE, S.-H. AND TERZOPOULOS, D. 2006. Heads up!: biomechanical modeling and neuromuscular control of the neck. In *SIGGRAPH Computer Graphics*. 1188–1198.
- LEE, Y., TERZOPOULOS, D., AND WALTERS, K. 1995. Realistic modeling for facial animation. In *SIGGRAPH Computer Graphics*. 55–62.
- LEMOIS, R., EPSTEIN, M., HERZOG, W., AND WYVILL, B. 2001. Realistic skeletal muscle deformation using finite element analysis. In *Proceedings of the XIV Brazilian Symposium on Computer Graphics and Image Processing*. 192–199.
- LEVEQUE, R. J. 2002. *Finite Volume Methods for Hyperbolic Problems*. Cambridge University Press.
- LEWIS, J. P., CORDNER, M., AND FONG, N. 2000. Pose space deformation: a unified approach to shape interpolation and skeleton-driven deformation. In *SIGGRAPH '00: Proceedings of the 27th annual conference on Computer graphics and interactive techniques*. ACM Press/Addison-Wesley Publishing Co., New York, NY, USA, 165–172.
- MA, Y.-Y., ZHANG, H., AND JIANG, S.-W. 2004. Realistic modeling and animation of human body based on scanned data. *J. Comput. Sci. Technol. 19*, 4, 529–537.
- MAGNENAT-THALMANN, N. 1985. *Computer animation: theory and practice*. Springer-Verlag New York, Inc., New York, NY, USA.
- MIN, K.-H., BAEK, S.-M., LEE, G., CHOI, H., AND PARK, C.-M. 2000. Anatomically-based modeling and animation of human upper limbs. In *Proceedings of International Conference on Human Modeling and Animation*.
- MOCCOZET, L. AND THALMANN, N. M. 1997. Dirichlet free-form deformations and their application to hand simulation. In *CA '97: Proceedings of the Computer Animation*. IEEE Computer Society, Washington, DC, USA, 93.
- MOONEY, M. 1940. A theory of large elastic deformation. *Journal of Applied Physics 11*, 582–592.
- NEALEN, A., MUELLER, M., KEISER, R., BOXERMAN, E., AND CARLSON, M. 2006. Physically based deformable models in computer graphics. *Computer Graphics Forum 25*, 4 (December), 809–836.
- NEDEL, L. P. AND THALMANN, D. 1998. Real time muscle deformations using mass-spring systems. In *Proceedings of Computer Graphics International*. IEEE.
- NG-THOW-HING, V. 2001. Anatomically-based models for physical and geometric reconstruction of humans and other animals. Ph.D. thesis, University of Toronto, Toronto, Canada.
- NG-THOW-HING, V. AND FIUME, E. 1999. B-spline solids as physical and geometric muscle models for musculoskeletal systems. In *Proceedings of the VIIth International Symposium of Computer Simulation in Biomechanics*. 68–71.
- NOCEDAL, J. AND WRIGHT, S. J. 2006. *Numerical Optimization*. Springer-Verlag.
- OOMENS, C. W. J., MAENHOUT, M., OIJEN, C. H. V., DROST, M. R., AND BAAIJENS, F. P. 2003. Finite element modelling of contracting skeletal muscle. *Philosophical Transactions: Biological Sciences 358*, 1453–1460.
- PANDY, M. G., ZAJAC, F. E., SIM, E., AND LEVINE, W. S. 1990. An optimal control model for maximum-height human jumping. *Journal of biomechanics 23*, 1185–1198.
- PARK, S. I. AND HODGINS, J. K. 2006. Capturing and animating skin deformation in human motion. *ACM Trans. Graph. 25*, 3, 881–889.
- PARK, S. I. AND HODGINS, J. K. 2008. Data-driven modeling of skin and muscle deformation. *ACM Trans. Graph. 27*, 3, 1–6.
- PRESS, W. H., FLANNERY, B. P., TEUKOLSKY, S. A., AND VETTERLING, W. T. 1992. *Numerical Recipes in C: The Art of Scientific Computing*. Cambridge University Press.
- SAND, P., MCMILLAN, L., AND POPOVIĆ, J. 2003. Continuous capture of skin deformation. *ACM Trans. Graph. 22*, 3, 578–586.
- SCHEEPERS, F., PARENT, R. E., CARLSON, W. E., AND MAY, S. F. 1997. Anatomy-based modeling of the human musculature. In *SIGGRAPH Computer Graphics*. 163–172.
- SEO, H. AND MAGNENAT-THALMANN, N. 2003. An automatic modeling of human bodies from sizing parameters. In *I3D '03: Proceedings of the 2003 symposium on Interactive 3D graphics*. ACM, New York, NY, USA, 19–26.
- SINGH, K. AND FIUME, E. 1998. Wires: a geometric deformation technique. In *SIGGRAPH '98: Proceedings of the 25th annual conference on Computer graphics and interactive techniques*. ACM, New York, NY, USA, 405–414.
- SLOAN, P.-P. J., ROSE, III, C. F., AND COHEN, M. F. 2001. Shape by example. In *I3D '01: Proceedings of the 2001 symposium on Interactive 3D graphics*. ACM, New York, NY, USA, 135–143.
- STERN, J. T. 1974. Computer modelling of gross muscle dynamics. *Journal of biomechanics 7*, 5, 411–28.
- STRANG, G. AND FIX, G. 2008. *An Analysis of the Finite Element Method 2nd Edition*. Wellesley-Cambridge.
- SUEDA, S., KAUFMAN, A., AND PAI, D. K. 2008. Musculotendon simulation for hand animation. *ACM Trans. Graph. 27*, 3, 1–8.
- TANG, C., ZHANG, G., AND TSUI, C. 2009. A 3d skeletal muscle model coupled with active contraction of muscle fibres and hyperelastic behaviour. *Journal of biomechanics 42*, 7, 865–872.
- TERAN, J., BLEMKER, S., HING, V. N. T., AND FEDKIW, R. 2003. Finite volume methods for the simulation of skeletal muscle. In *SCA '03: Proceedings of the 2003 ACM SIGGRAPH/Eurographics symposium on Computer animation*. 68–74.
- TERAN, J., SIFAKIS, E., BLEMKER, S. S., NG-THOW-HING, V., LAU, C., AND FEDKIW, R. 2005. Creating and simulating skeletal muscle from the visible human data set. *IEEE Transactions on Visualization and Computer Graphics 11*, 3, 317–328.
- THALMANN, D., SHEN, J., AND CHAUVINEAU, E. 1996. Fast realistic human body deformations for animation and vr applications. In *CGI '96: Proceedings of the 1996 Conference on Computer Graphics International*. 166–174.
- TSANG, W., SINGH, K., AND FIUME, E. 2005. Helping hand: an anatomically accurate inverse dynamics solution for unconstrained hand motion. In *SCA '05: Proceedings of the 2005 ACM SIGGRAPH/Eurographics symposium on Computer animation*. 319–328.

- TU, X. AND TERZOPOULOS, D. 1994. Artificial fishes: physics, locomotion, perception, behavior. In *SIGGRAPH Computer Graphics*. 43–50.
- UMBERGER, B. R., GERRITSEN, K. G. M., AND MARTIN, P. E. 2003. A model of human muscle energy expenditure. *Computer Methods in Biomechanics and Biomedical Engineering* 6, 2, 99–111.
- VERONDA, D. AND WESTMANN, R. 1970. Mechanical characterization of skin-finite deformations. *Journal of biomechanics* 3, 1, 111–124.
- WILHELMS, J. 1997. Animals with anatomy. *IEEE Comput. Graph. Appl.* 17, 3, 22–30.
- WILHELMS, J. AND VAN GELDER, A. 1997. Anatomically based modeling. In *SIGGRAPH Computer Graphics*. 173–180.
- WU, F. T., NG-THOW-HING, V., SINGH, K., AGUR, A. M., AND MCKEE, N. H. 2007. Computational representation of the aponeuroses as nurbs surfaces in 3d musculoskeletal models. *Computer Methods and Programs in Biomedicine* 88, 2, 112–122.
- WYVILL, B. AND WYVILL, G. 1989. Field functions for implicit surfaces. *The Visual Computer* 5, 1–2, 75–82.
- YUCESOY, C. A., KOOPMAN, B. H., HUIJING, P. A., AND GROOTENBOER, H. J. 2002. Three-dimensional finite element modeling of skeletal muscle using a two-domain approach: linked fiber-matrix mesh model. *Journal of biomechanics* 35, 9, 1253–1262.
- ZAHALAK, G. I. 1981. A distribution-moment approximation for kinetic theories of muscular contraction. *Mathematical Biosciences* 55, 1–2, 89–114.
- ZAJAC, F. E. 1989. Muscle and tendon: properties, models, scaling, and application to biomechanics and motor control. *Crit Rev Biomed Eng* 17, 4, 359–411.
- ZAJAC, F. E. AND GORDON, M. 1989. Determining muscle's force and action in multi-articular movement. *Exercise and Sport Sciences Reviews* 17, 187–230.
- ZHU, Q.-H., CHEN, Y., AND KAUFMAN, A. 2001. Real-time biomechanically-based muscle volume deformation using fem. *Computer Graphics Forum* 17, 3 (Dec.), 275–284.
- ZORDAN, V. B., CELLY, B., CHIU, B., AND DILORENZO, P. C. 2004. Breathe easy: model and control of simulated respiration for animation. In *SCA '04: Proceedings of the 2004 ACM SIGGRAPH/Eurographics symposium on Computer animation*. 29–37.